VOL. 17, NO. 14, JULY 2022 ISSN 1819-6608
ARPN Journal of Engineering and Applied Sciences

www.arpnjournals.com

A SYSTEMATIC STUDY OF THE STRUCTURAL AND MAGNETIC PROPERTIES OF NICKEL DOPED α-Fe_2O_3 NANOPARTICLES PREPARED FROM LOGAS NATURAL SAND

Erwin Amiruddin[1], Salomo Sinuraya[1], Rahmondia N. Septiadi[1], Yanuar Hamzah[1], Amir Awaluddin[2], Loly A. Hardani[3], Fitri A. Lestari[3], Yessi Magdalena[3] and Devi T. Gurning[3]
[1]Department of Physics, Faculty of Mathematics and Natural Sciences, Riau University, Pekanbaru, Indonesia
[2]Department of Chemistry, Faculty of Mathematics and Natural Sciences, Riau University, Pekanbaru, Indonesia
[3]Magnetic Laboratory, Faculty of Mathematics and Natural Sciences, Riau University, Indonesia
E-Mail: erwin_amiruddin@yahoo.com

ABSTRACT

The nickel doped iron oxide nanoparticles type hematite (α-Fe_2O_3) have been prepared by ball milling method using Logas natural sand as a raw material. The hematite nanoparticles were doped using nickel with concentration of 0, 5, 10 wt.% and characterized by vibration sample magnetometer (VSM), X-ray diffractometer (XRD), scanning electron microscopy (SEM) and X-ray fluorescence (XRF) spectroscopy. The magnetic measurement demonstrate that magnetic properties are strongly depend on nickel content and revealed that all of the samples exhibited weak ferromagnetic behaviour with the coercivity ranged from 336 Oe to 357 Oe. The XRD measurements confirmed the formation of crystalline, rhombohedral crystal structure and α-Fe_2O_3 nanoparticles. Nickel doped samples show nickel-hematite phase as indicated through XRD measurement. The average crystallite size calculated based on Scherrer formula found to be 31.73, 29.09 and 28.38 nm after being doped with nickel 0, 5 and 10 wt.%, respectively which are consistent with the results obtained from SEM images. Some other elements such as aluminium, silicon and titanium and others elements were detected using X-Ray Fluorescence Spectroscopy (XRF), which demonstrates that these milled samples are not purely hematite.

Keywords: hematite, logas natural sand, nickel doped, ball milling, magnetic properties.

INTRODUCTION

Nowadays, iron oxide nanoparticles have attracted great attention for research compared to many metal oxide nanoparticle types. This is due to their wide range applications started from catalysts [1, 2] to biomedical applications [3, 4] and environmental remediation [5]. There are several available methods for preparing α-Fe_2O_3 nanoparticles such as solvo thermal, [6] laser pyrolysis, [7] thermal oxidation, [8] hydrothermal [9] methods. However, the simplest way to prepare hematite nanoparticles is ball milling method [10]. It was observed that iron oxide nanoparticles show very different physical and chemical properties depending on their microstructure, such as size uniformity and crystallinity. Therefore, preparing magnetic nanoparticles that can maintain size uniformity and crystallinity is important.

Among the reported iron oxides, the hematite α-Fe_2O_3 seem to be more popular because of their chemical stability under ambient conditions and exhibits various interesting properties such as high surface to volume ratios and superparamagnetic behaviour [11]. Super paramagnetic iron oxide nanoparticles have a large magnetic moment and very small coercivity. For environmental applications, hematite (α-Fe_2O_3) are preferable and known as the highly recommended iron oxide due to their small band gap energy (2.1 eV) [12] and have ability to absorb visible light. However, there are still some limitations that need to be addressed for α-Fe_2O_3 nanoparticles before applying them as photocatalyst. Therefore, several strategies have been developed to reduce the band energy of this type of iron oxide. One of them is by doping hematite nanoparticles using different materials such as transition metal elements [13]. Choice of doping elements of iron oxide nanoparticles determines the extent of modification in properties. For example, previous researcher [14] used Sn, Nb, Pt, Zr, Ti, Zn and Ni cations to modify magnetic, structural as well as morphology of hematite nanoparticles using ball milling. Similar modifications have been reported for iron oxide using manganese [15]. This modification may have the ability to control Mn/Fe ratio and thus may change the structural and magnetic properties of iron oxide nanoparticles and therefore can optimize them for catalyst application.

To enhance some specific properties such as magnetic properties of hematite, we report the effect of undoped and nickel doped hematite nanoparticles on their magnetic, structural and morphological properties prepared using ball milling method. The properties of hematite nanoparticles are correlated with variation in nickel concentration (wt.%).

EXPERIMENTAL PROCEDURE

Raw Material

The starting material to prepare the hematite (α-Fe_2O_3) was natural sand from Logas district-Kuansing Regency - Riau Province. Indonesia. Nickel powder (99.99%) was bought from Toko Pedia (www.tokopedia.com).

Preparation of Undoped and Nickel Doped α-Fe_2O_3 Nanoparticles

Hematite nanoparticles were prepared from Logas natural sand, Kuansing Regency Riau Province using ball milling method. Sample of natural sand were dried prior to iron sand separator (ISS) process. The iron oxide particles of ISS product was separated again from non iron oxide particles using NdFeB magnet. This product was milled for 120 hours and then processed again using NdFeB. The ball milling products called BMA, BMB, BMC and BMD were doped with nickel in concentration of 0, 5, 10 and 15%, respectively. The powder of nickel and iron oxide nanoparticles were mixed and milled for 20 hours. These products were studied for their magnetic, structural and morphological properties as well as product composition using vibration sample magnetometer (VSM), X-Ray Diffractometer (XRD), and Scanning Electron Microscope (SEM) as well as X Ray Fluorescence (XRF) Spectroscopy.

RESULTS AND DISCUSSIONS

X-Ray Diffraction Analysis

Structural properties of undoped and nickel doped α-Fe_2O_3 nanoparticles were analyzed using X-Ray Diffractometer Phillips producing CuKα radiation with wavelength of 0.15406 nm. In this measurement, the diffraction angle was selected in interval of 10° to 100° with the step of 0.01°. The diffraction peaks of undoped sample are shown at diffraction angles of 23.8932°, 32.7516°, 35.3642°, 40.4855°, 49.0172°, 53.4487°, 61.8377° and 63.4875° are completely matched the reflections of (102), (104), (110), (113), (024), (116), (018), and (214), respectively as shown in Figure-1. The as prepared undoped α-Fe_2O_3 nanoparticles has a hexagonal structure [16]. The observed diffraction peaks of the undoped α-Fe_2O_3 nanoparticles are in good agreement with the diffractions peaks of the α-Fe_2O_3 (JCPDS no. 89-8103). In the case of 5 and 10 wt.% nickel doped α-Fe_2O_3 nanoparticle, the diffraction patterns of α-Fe_2O_3 nanoparticles show that their structure is not changed with nickel doping. The XRD patterns show additional peaks at diffraction angle of 44.51° and 51.93° with correspond to reflection planes of (111) and (200), respectively which are characteristic of nickel (JCPDS no. 04-850) [17]. The intensity of the reflection of nickel phase increases as nickel content increase which reveals the dominant presence of nickel phase in the samples. Therefore, the existence of diffraction peaks related to the nickel and α-Fe_2O_3 nanoparticles showed successful formation of α-Fe_2O_3-nickel nanoparticles using ball milling method. It also can be noticed from Figure-1 that small shift of the diffraction peaks occurs in most peak positions to slightly lower angles are observed for nickel doped samples. This shift of peak positions to slightly lower angles is shown in the inset patterns for the expanded diffraction angle of 32° - 34°. This finding can be explained due to the milling and the formation of the nickel phase in the samples [18]. The average crystallite size affects the diffraction peaks and therefore, Scherrer formula [19] was used to calculate the crystallite size for the undoped and nickel doped samples. The average crystallite size of the samples as shown in Table-1 is 31.73, 29.09 and 28.38 nm for undoped (0 wt.%), 5 wt.% and 10 wt.% nickel doped samples, respectively. The decrease of average crystallite sizes of hematite nanoparticles with increasing nickel concentration could be due to the nickel atoms located surround hematite nanoparticles boundaries and therefore, decrease the diffusion rate [20]. Therefore, the average crystallite size of nickel-doped hematite nanoparticles become smaller compared to that of the undoped hematite nanoparticles. In order to compare our results with the literature, we used all the planes in the diffraction pattern to calculate the size of the α-Fe_2O_3 crystallite. The results obtained agree with the data in the literature in which the crystallite sizes between 21 and 82 nm [21].

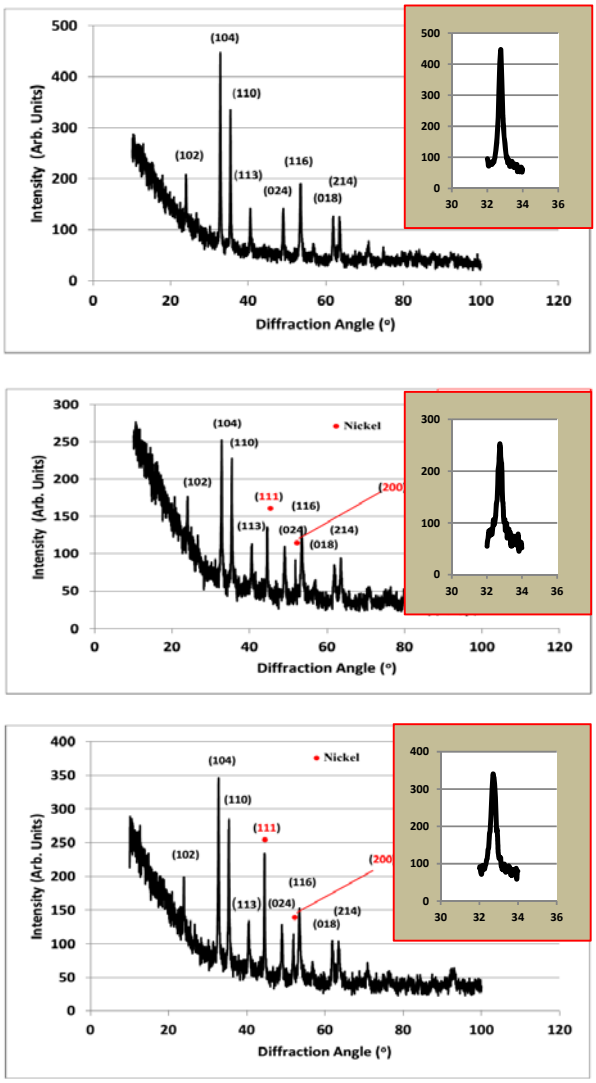

Figure-1. XRD patterns (a) undoped and (b) 5 wt.% and (c) 10 wt.% nickel doped α-Fe_2O_3 nanoparticles. The inset patterns show the expanded diffraction angle of 32°-34° showing shift of peak position to slightly lower angle.

Table-1. The average crystallite size of undoped and nickel doped hematite nanoparticles.

Nickel Content (wt.%)	Average Crystallite size (nm)
0 (undoped)	31.73
5	29.09
10	28.38

Elemental chemical composition of Logas natural sand before and after milling process as well as after being 5 wt.% doped nickel determined using X-Ray Fluorescence Spectroscopy (XRF) is presented in Figure-2. It can be seen that the XRF data clearly evidence the occurrence of the doping elements. The figure also indicates that the α-Fe_2O_3 nanoparticles are not free from impurity elements. The Fe contents were increased very significantly after milling (120 hours). Some other elements for examples Al, Si, and other elements were decreased, however, the other elements such as Ti increases. This indicates that natural sand grains break into smaller parts so that the non-magnetic and magnetic grains were separated during milling process. Moreover, Fe and Ti elements cannot be separated until 120 hours milling process suggesting that Fe and Ti exist in the form of compound.

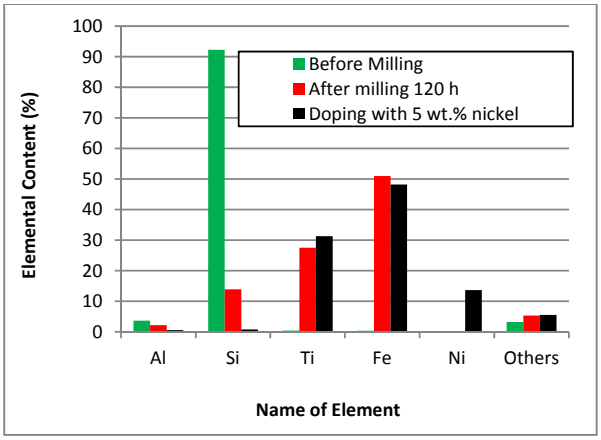

Figure-2. Elemental chemical composition of sample before and after being milled for 120h and after being 5 wt.% doped nickel observed by XRF.

Magnetic Properties

The hysteresis loops of the undoped and nickel doped α-Fe_2O_3 nanoparticles measured using VSM are shown in Figure-3. The applied magnetic field used was ranging from +20.000 Oe to -20.000 Oe. It is obvious that the saturation magnetization value of the samples increases as the concentration of nickel increase which might be because of the presence of more nickel atoms at the grain boundaries as revealed in the X-Ray Diffraction (XRD) results [22]. The increase in saturation magnetization values is associated with a reduction in the crystallite size. Similar results of increased magnetizations after being nickel doped nickel doped α-Fe_2O_3 nanoparticles have also been reported by other researchers [23] and they conclude that the increase in saturation magnetization for nickel doped α-Fe_2O_3 nanoparticles is due to the higher surface spins of electrons. Similar results of increased magnetizations after being nickel doped nickel doped α-Fe_2O_3 nanoparticles have also been reported by other researchers [24]. The coercivity of the undoped α-Fe_2O_3 nanoparticles is found to be 336.21Oe and it increases for the 5 wt.% and 10 wt.% nickel doped α-Fe_2O_3 nanoparticles to 354.05 Oe and 357.61 Oe, respectively as indicates in Table-2. It is clearly noticed that the hysteresis loops of all samples show weak ferromagnetic behavior characterized by their low coercivity. The undoped hematite nanoparticles show the remanent magnetization (M_r) of 2.71 emu/g and it decreases for the 5 wt.% and 10 wt.% nickel doped samples to about 3.24 and 3.36 emu/g, respectively. It can be seen from Figure-3(c) that as increasing nickel doping concentration, the loop squareness increases from 0.200 to 0.215. This shows that tuning of magnetic properties is possible by doping the hematite with nickel.

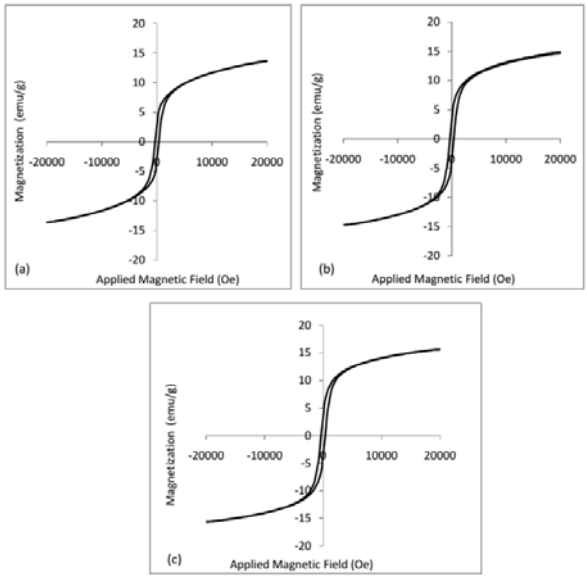

Figure-3. Hysteresis loops of (a) undoped (b) 5 wt.% nickel doped and (c) 10 wt.% nickel doped hematite nanoparticles.

Table-2. Magnetic parameters of the undoped and nickel doped α-Fe_2O_3 nanoparticles.

Nickel Content (%)	Ms (emu/g)	Hc (Oe)	Mr (emu/g)	S (Mr/Ms)
0	13.57	336.21	2.71	0.200
5	14.83	354.05	3.24	0.211
10	15.61	357.61	3.36	0.215

Scanning Electron Microscope (SEM) Results

The surface morphological study of the undoped and nickel doped α-Fe_2O_3 nanoparticles was carried out using SEM. Figure-4 shows the SEM micrographs of the undoped and nickel doped α-Fe_2O_3 nanoparticles. SEM images show that the size of the nanoparticles differs slightly by changing the concentration of dopant and the particles are irregular in shape and randomly organized. Moreover, no significant morphological differences between undoped and nickel doped hematite nanoparticles can be viewed by comparing the micrographs of undoped and nickel doped one. However, SEM micrograph of undoped α-Fe_2O_3 nanoparticles undergoes agglomeration. This is due to magnetic interaction between α-Fe_2O_3 nanoparticles. The SEM images of nickel doped α-Fe_2O_3 nanoparticles also show the agglomerated form which is believed due to the high surface energies possessed by α-Fe_2O_3 nanoparticles [25]. The average particle size estimated from these images for undoped, 5 wt.% and 10 wt.% nickel doped hematite nanoparticles is roughly 128, 131, and 133 nm. In line with XRD results, which revealed the average particles size is much bigger than that compared to determined by XRD and this is due to XRD analysis only discussed about single crystallite size. The effect of nickel on morphology identified from this study can be used to understand the magnetic properties of iron oxide nanoparticles.

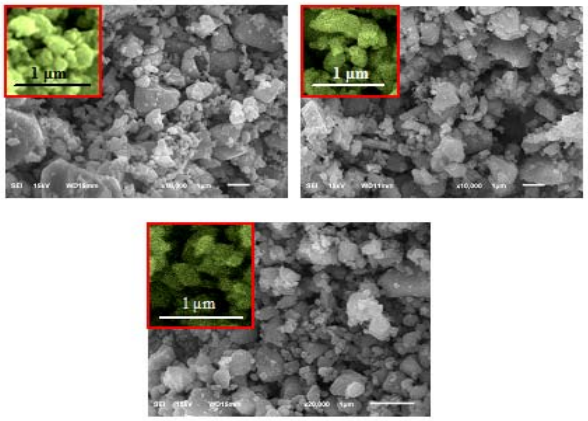

Figure-4. SEM micrographs of (a) undoped, (b) 5 wt.% nickel doped and (c) 10 wt.% nickel doped α-Fe_2O_3 nanoparticles. The inset micrograph shows the expanded morphology of the samples.

CONCLUSIONS

In this study, we have investigated the magnetic, structural and morphological properties of undoped and nickel-doped hematite (α-Fe_2O_3) nanoparticles with various content of nickel (0 wt.%%, 5 wt.%, and 10 wt.%) using ball milling method. It is found that the substitution of nickel nanoparticles can cause a significant change in the magnetic, structural and morphological properties of the α-Fe_2O_3. The XRD result confirmed that the prepared samples are crystalline with size in nanoscale. Nickel doped samples show nickel-hematite particles as indicated through XRD measurement. The crystallite size of hematite nanoparticles calculated based on Scherrer formula decreases with increasing nickel content. The size of hematite nanoparticles decreased as nickel content increases according to SEM images. These results are interesting and may apply on a further experimental investigation of the nickel doped α-Fe $_2O_3$ as a low-cost and high photo catalytic activity material.

ACKNOWLEDGMENTS

This work was supported by the Directorate General of Higher Education (DGHE), Indonesian Ministry of Education and Culture, 2021. The authors are grateful to Physics department UNP for XRD and XRF measurements and department of Chemistry ITB for SEM measurement as well as to Indonesian Sciences Institute (LIPI) for conducting the VSM measurement. Many thanks go to magnetic research members in Magnetism Laboratory FMIPA UNRI for their assistance during sample collection and preparation.

REFERENCES

[1] Zhiqin Cao, Mingli Qin, Yueru Gu, Baorui Jia, Pengqi Chen, Xuanhui Qu. 2016. Synthesis and characterization of Sn doped hematite as visible light photocatalyst, Mater. Res. Bull. 77: 41-47.

[2] Nguyen C. C., Vu N. N., Do T. O. 2015. Recent Advances in the Development of Sunlight-Driven Hollow Structure Photocatalysts and their Applications. J. Mater. Chem. A. 3: 18345-18359.

[3] Colombo M., Carregal-Romero S., Casula M.F., Gutierez L., Morales M.P., Bohm I.B., Heverhagen J.T., Prosperi D., Parak W.J. 2012. Biological applications of magnetic nanoparticles. Chem. Soc. Rev. 41, 4306-4334.

[4] Singamaneni S., Bliznyuk V. N., Binek C., Tsymbal E.Y. 2011. Magnetic nanoparticles: Recent advances in synthesis, self-assembly and applications. J. Mater. Chem. 21: 16819-16845.

[5] Pegu R, Majumdar KJ, Talukdar DJ, Pratihar S. 2014. Oxalate capped iron nanomaterial: from methylene blue degradation to bis (indolyl) methane synthesis. Rsc Advances. 4: 33446-33456.

[6] Zhu D, Zhang J, Song J, Wang H, Yu Z, Shen Y, Xie A. 2013. Efficient one-pot synthesis of hierarchical flower-like α-Fe_2O_3 hollow spheres with excellent adsorption performance for water treatment. Appl Surf Sci. 284: 855-61.

[7] Dumitrache F, Morjan I, Fleaca C, Badoi A, Manda G, Pop S,Marta DS, Huminic G, Huminic A, Vekas L, Daia C, Marinica O, Luculescu C, Niculescu AM. 2015. Highly magnetic Fe_2O_3 nanoparticles synthesized by laser pyrolysis used for biological and heat transfer applications. Appl. Surf Sci. 336: 297-303.

[8] Su X, Yu C, Qiang C. 2011. Synthesis of α-Fe_2O_3 nano-belts and nanoflakes by thermal oxidation and study to their magnetic properties. Appl Surf Sci. 257: 9014-8.

[9] Tadica M, Panjan M, Damnjanovicc V, Milosevic I. 2014. Magnetic properties of hematite (α-Fe_2O_3) nanoparticles prepared by hydrothermal synthesis method. Appl Surf Sci. 320:183-7.

[10] Erwin Amiruddin, Amir Awaluddin, Innike Hariani, Ribka Sihombing and Riska Angraini. 2020. The Influence of Milling Ball Size on the Structural, Morphological and Catalytic Properties of Magnetite (Fe_3O_4) Nanoparticles toward Methylene Blue Degradation. Journal of Physics: Conference Series 1655: 012006, doi:10.1088/1742-6596/1655/1/012006

[11] Xu P., Zeng G.M., Huang D.L., Feng, C.L., Hu S., Zhao M.H., Lai C., Wei Z., Huang C., Xie G.X., Liu Z.F. 2012. Use of iron oxide nanomaterials in wastewater treatment: A review. Sci. Total Environ. 2012: 424, 1-10.

[12] L. Li, Y. Yu, F. Meng, Y. Tan, J. R. Hamers, and S. Jin. 2012. Facile Solution Synthesis of α-$FeF_3 \cdot 3H_2O$ Nanowires and Their Conversion to α-Fe_2O_3 Nanowires for Photo-electrochemical Application. Nano Lett. 12: 724.

[13] Caia L, Hua Z, Brantonb P. 2014. The effect of dopingtransition metal oxides on copper manganese oxidesfor the catalytic oxidation of CO Chinese J Catal. 35: 159-167.

[14] Malviya K D, Dotan H, Shienkevich D, Tsyganok A, Mor H and Rothschild A. 2016. Systematic comparison of different dopantsin thin films hematite (α-Fe_2O_3) photo anode for solar water splitting J. Mater. Chem. A. 4: 3091-3099.

[15] Erwin Amiruddin, Amir Awaluddin, Salomo Sinuraya, Heri Hadianto, Muhammad Deri Noferdi and Ainun Syarifatul Fitri. 20121. Study of Iron Oxide Nanoparticles Doped with Manganese for Catalytic Degradation of Methylene Blue. Journal of Physics: Conference Series. 2049: 012021, doi: 10.1088/1742-6596/2049/1/012021.

[16] K. Supattarasakda, K. Petcharoen, T. Permpool, A. Sirivat, W. Lerdwijitjarud. 2013. Control of hematite nanoparticle size and shape by the chemical precipitation method. Powder Technol. 249: 353-359.

[17] Amrut S. Lanje, Satish J. Sharma and Ramchandra B. Pode. 2010. Magnetic and Electrical Properties of Nickel Nanoparticles prepared by Hydrazine Reduction Method. Scholars Research Library, Archives of Physics Research. 1(1): 49-56.

[18] O. M. Lemine, Ghiloufi, M. Bououdina, L. Khezami, M. M'hamed and A. Taha. 2013. Nanocrystalline Ni doped α-Fe2O3 for Adsorption of Metals from Aqueous Solution. doi: http://dx.doi.org/10.1016 /j.jallcom.2013.10.202.

[19] J. Lin, Y. Lin. 2002. Hot-fluid annealing for crystalline titanium dioxide nanoparticles in stable suspension, J. Am. Chem. Soc. 124, 11514–11518, doi:http://dx.doi.org/10.1021/ja0206341. 12236766

[20] Svetlana Em, Mussa Yedigenov, Laura Khamkhash, Anara Molkenova, Timur Sh. Atabaev. 2020. Sn Doped Hematite Nanoparticles for Potential Photocatalytic Dye Degradation. IOP Conf. Series: Materials Science and Engineering 739, 012042 doi:10.1088/1757-899X/739/1/012042

[21] Lassoued A., Dkhil B., Gadri A., Ammar S. 2017. Control of theshape and size of iron oxide (α-Fe_2O_3) nanoparticles synthesized through the chemical precipitation method. Results Phys. 7: 3007-3015.

[22] Erwin Amiruddin, Heri Hadianto, Martha Riana, Salomo Sinuraya, Mohammad Deri Noverdi and Ainun Syarifatul Fitri. 2021. Undoped and manganese doped iron oxide nanoparticles for environmental applications. ARPN Journal of Engineering and Applied Sciences. 16(18): 1872-1876.

[23] S. Sivakumar, D. Anusuya, Chandra Prasad Khatiwada, J. Sivasubramanian, A. Venkatesan, P. Soundhirarajan. 2014. Characterizations of diverse mole of pure and Ni-doped α-Fe_2O_3 synthesized nanoparticles through chemical precipitation route. Spectrochimica Acta Part A: Molecular and Biomolecular Spectroscopy. 128: 69-75.

[24] E. Darezereshki. One-step synthesis of hematite (α-Fe_2O_3) nano-particles by direct thermal-

decomposition of maghemite Mater. Lett. 2011: 65 642-645.

[25] S. Sagadevana, Z. Z. Chowdhury and R. F. Rafiquec. 2018. Preparation and Characterization of Nickel ferrite Nanoparticles via Co-precipitation Method. Materials Research. 21, DOI: 10.1590/1980-5373-MR-2016-0533